BOREAL ENVIRONMENT RESEARCH 10: 323–336 ISSN 1239-6095
Helsinki 24 October 2005

Formation and growth of fresh atmospheric aerosols: eight years of aerosol size distribution data from SMEAR II, Hyytiälä, Finland

Miikka Dal Maso[1)], Markku Kulmala[1)], Ilona Riipinen[1)], Robert Wagner[1)], Tareq Hussein[1)], Pasi P. Aalto[1)] and Kari E. J. Lehtinen[2)]

[1)] *Division of Atmospheric Sciences, Department of Physical Sciences, P.O. Box 64, FI-00014 University of Helsinki, Finland*
[2)] *Finnish Meteorological Institute and University of Kuopio, Department of Applied Physics, P.O. Box 1627, FI-70211 Kuopio, Finland*

Dal Maso, M., Kulmala, M., Riipinen, I., Wagner, R., Hussein, T., Aalto, P. P. & Lehtinen, K. E. J. 2005: Formation and growth of fresh atmospheric aerosols: eight years of aerosol size distribution data from SMEAR II, Hyytiälä, Finland. *Boreal Env. Res.* 10: 323–336.

We analyzed size distributions measured continuously at a boreal forest measurement site at Hyytiälä, Finland between 1996 and 2003. From the eight-year data we identified days when new aerosol particle formation was taking place as well as days when no formation was detected, removing days with ambiguous status. The event days were then classified based on whether it was possible to determine formation and growth rates of new particles. These characteristics were then calculated. We found that new particle formation happens frequently in the boreal forest boundary layer, with at least 24% of days containing an event. Events are more probable during spring and autumn than during other times of the year. The average formation rate of particles larger than 3 nm was 0.8 cm^{-3} s^{-1}, with enhanced rates during spring and autumn. The mean growth rate was 3.0 nm h^{-1}, peaking in summer. The created event database is valuable for future studies of reasons leading to new particle formation in the atmosphere.

Introduction

The radiative balance of the Earth is affected by the absorbing, scattering and cloud condensation nuclei (CCN) forming properties of atmospheric aerosols. The magnitude of the aerosol radiative forcing, however, is associated with large uncertainties, partly because the sources of atmospheric aerosols are unknown.

Development of instrumental techniques to measure aerosol size distributions to the smallest sizes has enabled scientists to understand the formation of secondary aerosol particles. During the recent decade, observations made in various environments and sites all around the world have shown that new secondary particle formation bursts occur frequently in the Earth's atmosphere (Kulmala *et al*. 2004). Such observations span from northernmost sub-arctic Lapland, the remote boreal forest (Mäkelä *et al*. 1997, Kulmala *et al*. 1998), heavily populated urban sites (Mönkkönen *et al*. 2005), Antarctic areas (Koponen *et al*. 2003), the coastal boundary layer (O'Dowd *et al*. 2002) to industrialized agricultural regions in Germany (Birmili and Wiedensohler 2000). Common to all these meas-

urements is that they show episodes of ultrafine aerosol particles appearing in the atmosphere and subsequently growing to larger sizes, potentially until they reach sizes where they can have a climatic impact by scattering solar irradiation or indirectly by functioning as cloud condensation nuclei.

The observations made are, however, often made during measurement campaigns, and the scientific community lacks data from long-term, continuous measurements. Such measurements are valuable to assess the impact of new particle formation, allowing scientists to quantify the influx of aerosol due to secondary aerosol formation. In conjunction with measurements of other atmospheric properties, long-term measurements also enable studies into the dynamics of secondary aerosol formation and present control data for climate modelers trying to predict future climatic conditions.

Measurements of ambient aerosol size distributions were started at the SMEAR II station at Hyytiälä, Finland, in January 1996, and have been ongoing since then. In this study we analyze these size distribution data to identify periods of new particle formation and growth, as well as days when no particle formation is observed. We define simple criteria for event occurrence, and use them on an eight-year period of measured data. We also identify event days when it is possible to quantify rates of particle appearance and growth as well as other parameters describing the aerosol dynamics during the formation event. The annual variation of the results is studied to find seasonal differences in new particle occurrence. Previous studies of particle formation days have concentrated only on days where particle formation was observed, often using a classification system to describe the strength and continuity of the burst (Mäkelä *et al*. 2000b, Boy and Kulmala 2002). However, when making point measurements in the atmosphere where local and regional sources are contributing to the measured aerosol, it is often a matter of some dispute whether a certain day exhibits particle formation. Given that the particle formation process is still unknown, combined with the nature of atmospheric measurements, we think it unlikely to find an exact dividing line between the formation and no-formation days. For a statistical analysis it is, however, important to separate particle formation days from days with no formation.

The new particle formation burst classification we present here is straightforward and uses well-defined guidelines to identify new particle formation periods. In addition, it separates particle formation days from days with no particle formation. With this new classification, combined with improved analysis methods and an exceptionally long dataset, we aim to provide scientists with a database that will help to shed light on the causes and magnitude of secondary aerosol particle formation in the boreal forest.

Site description and instrumentation

The boreal forest ecosystem measurement station SMEAR II (System for Measuring Forest Ecosystem–Atmosphere Relationships II) is a cross-disciplinary co-operation platform for atmospheric sciences, soil chemistry and forest ecology to investigate various fluxes of different compounds in a Scots pine forest (e.g. Hari and Kulmala 2005). The main research subjects at the station are gaseous and particulate pollutants and their role in cloud formation, the impact of environment and tree structure on gas exchange, water transport and the growth of trees, and budgets of various substances of the soil.

The station is located at Hyytiälä, southern Finland (61°51´N, 24°17´E, 170 m above sea level). The surrounding forest is a 42-year-old homogeneous pine forest extending several kilometers to the north and northeast. At a distance of about 1 km west of the station there is a small lake; the buildings of the station's infrastructure are located at the shore of the lake. The nearest urban locations are Tampere about 50 km to the south-west and Jyväskylä 100 km to the north-east.

The station is equipped with extensive facilities to measure forest ecosystem–atmosphere interactions. These include a 72-meter tower from which various trace gas concentrations, meteorological parameters (wind speed, temperature, relative humidity), various fluxes and irradiation are measured (Vesala *et al*. 1998, Kulmala *et al*. 2001b).

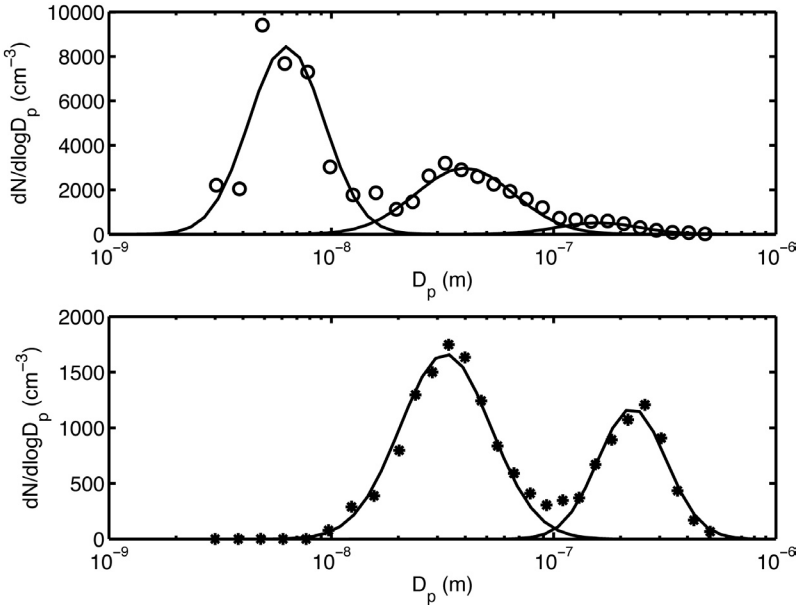

Fig. 1. Examples of measured size distributions at the SMEAR II station in Hyytiälä. The upper panel shows a size distribution with three modes, the nucleation (3–25 nm), Aitken (25–100 nm) and accumulation (> 100 nm) modes. The markers represent measured data points and the solid lines show the modes which were obtained with the automated fitting method of Hussein *et al.* (2005). The lower panel shows a bimodal size distribution with no nucleation mode particles.

Particle size distribution measurements are performed using a setup of two differential mobility particle sizers (DMPS) (Aalto *et al.* 2001). The DMPS system extracts a small electrical mobility increment from the sample air using a differential mobility analyzer (DMA) and transfers it to a condensation particle counter (CPC). The first DMPS measures particles with sizes between 3 and 10 nm; it consists of a Hauke-type DMA with a length of 10.9 cm and a TSI Model 3025 CPC. The second DMPS measures particles between 10 and 500 nm, consisting of a 28-cm DMA and a TSI Model 3010 CPC. The aerosol is neutralized with a 74 mBq (2 mCi) ^{85}Kr beta source. The sheath flows are maintained using a closed loop arrangement with critical orifices (Jokinen and Mäkelä 1997). The sampling is performed through the eastern wall of the measurement cottage, at a height of 2 m above the ground. The primary sample flow is ca. 25 m^3 h^{-1} of which the sample flow (2.5 l min^{-1}) is taken to the instrument. The size distributions of both DMPS systems are combined to obtain the size coverage of 3–500 nm. The time resolution of the combined system is 10 minutes, adding up to 144 size distributions daily.

The DMPS system was installed at the SMEAR II station in January 1996, with the purpose of obtaining regular background data of submicron aerosol size distributions. At the time new particle formation was thought to be probable but happening rarely in the atmosphere (Mäkelä *et al.* 1997); long time series were deemed necessary to observe the phenomenon with a good probability. Since then, the instrument has been running continuously. For this study we have selected the time period starting from 30 January 1996 and ending 31 December 2003, a total of 2892 days.

Size distribution analysis

The submicron size distributions measured at the SMEAR II station exhibited a modal structure with two or three modes, which were usually distributed log-normally. Characteristic features included the accumulation mode, covering a size range of 100–500 nm, which was present at practically all times. Usually a mode was present also in the size range of 25–100 nm, forming the Aitken mode. However, often we observed a third mode in the size range of 3–25 nm, called the nucleation mode (*see* examples in Fig. 1).

Instances where a new particle mode appeared in the sub-25-nm size range are considered to be caused by formation of new particles from precursor vapors (*see* for example Kulmala *et al.* 1998, 2001a). These particles usually subsequently grow, forming a nucleation mode

which evolves to larger sizes, sometimes reaching Aitken- or even accumulation-mode sizes. During these events, the transition between subsequent measured size distributions is usually smooth, with little change in other modal parameters than size. The fact that this holds for several hours — sometimes even days — despite horizontal advection we consider strong evidence of the particles being born over a large area (Kulmala *et al*. 1998).

Classifying new particle formation events

Instances of new particle formation (NPF) are frequently observed in the SMEAR II time series. To reliably determine the processes and atmospheric conditions leading to NPF events, we need information about the times when events were recorded and when no particles are formed. Using this information, it is later possible to analyze relevant atmospheric variables and correlate them with the NPF events. However, there exists no unique mathematical criterion or definition for an NPF event.

We analyzed the data visually on a day-to-day basis: each 24-hour period, from midnight to midnight, was classified according to whether it contained a new particle formation event. The classification was done in a three-person group to reduce subjective bias. For a day to be classified as an NPF event, the following criteria had to be met:

1. A distinctly new mode of particles must appear in the size distribution.
2. The mode must start in the nucleation mode size range.
3. The mode must prevail over a time span of hours.
4. The new mode must show signs of growth.

Using these criteria we aim to exclude new particle formation from point sources. This is justified by the need to separate local pollution sources, such as traffic or heating, which are capable of producing nucleation-mode particles, from the "natural" production of particles. We also explicitly state that an NPF event always involves particle growth. This is justified by the assumption that new particles are formed at sizes lower than our instrumentation's detection limit, and therefore growth is necessary for NPF to be observed at all.

It should be noted that our criteria are not applicable at sites where the assumption that particle formation occurs over a geographically wide area does not hold. For example at coastal sites such as Mace Head, Ireland, where NPF events happen at low tide when the algae on the beach are exposed (O'Dowd *et al*. 2002), NPF happens practically at a point or line source and does not show growth.

As well as events, also days with no particle formation are of interest for comparison and control purposes when studying reasons leading to NPF events. These days we called non-events. They are characterized by an absence of particles in the nucleation mode size range, mostly displaying a bimodal size distribution. However, a large number of days did not fulfill the criteria to be classified as either events or non-events. These included days with some sporadic occurrence of particles in the nucleation mode range, or days when we can see the later phase of a mode growing in the Aitken-mode size range. These days were classified as undefined; the purpose of this was to remove them from any analysis comparing event and non-event days.

Additional requirements are set for an NPF burst when we try to quantify basic characteristics such as the particle growth rate (GR) and formation rate (J_{nuc}). For this, the evolving size distribution is required to be well behaved, meaning that the nucleation mode should be clearly distinguishable for a long enough time, in our case for several hours. This is to ensure that we have enough data points for analysis as our instrument's time resolution is 10 minutes. To separate days when these characteristics could be derived from the size distributions with high confidence, we classified the NPF events into two classes (Fig. 2):

- Class I: Days when the growth and formation rate could be determined with a good confidence level,
- Class II: Days where the derivation of these parameters was not possible or the accuracy of the results was questionable.

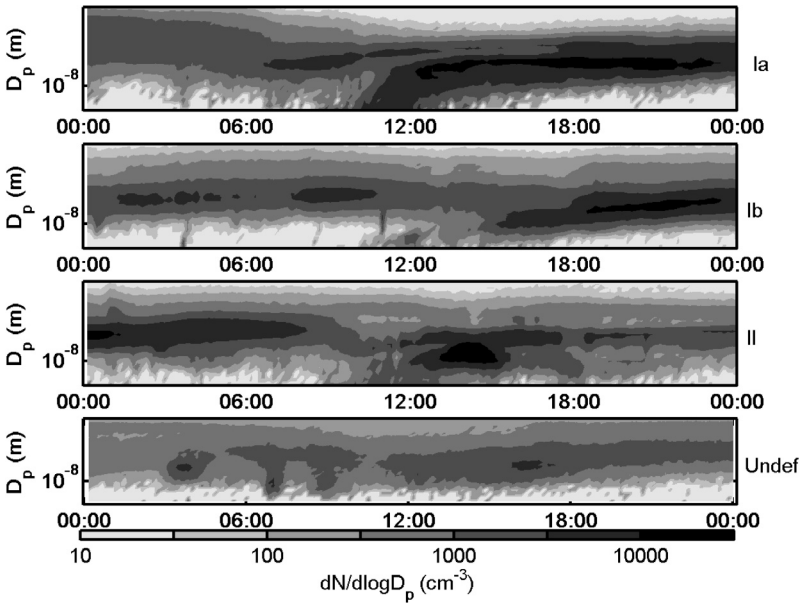

Fig. 2. Examples of particle formation bursts and their classification. The two upper-most panels show days with new particle formation events, for which we could obtain the growth and formation rates (class I events). The third panel shows an event where the growth rate determination was not successful (class II event). The lowest panel shows a day where ultrafine particles are present sporadically, but the day could not be clearly termed a particle formation event day (undefined).

Class I was divided into sub-classes Ia and Ib. Class Ia contains very clear and strong particle formation events, with little or no pre-existing particles obscuring the newly formed mode, making them suitable for modeling case studies of NPF events. Class Ib contains the rest of class I events.

The classification panel discussed each case to ensure the criteria were met. In cases where the panel could not agree whether the day should be classified as an event/non-event, the day was classified as "undefined". The days were first analyzed in sequence; after the initial classification the days were grouped according to their class, and re-evaluated. This was done to eliminate a possible "drift" in the evaluators' opinion.

Days when there was longer than a three-hour gap in the data we removed from the data pool as we could not be assured that no particle formation was happening during that period. However, if a day showed a clear particle formation burst, it was classified as such despite possible gaps in data.

A flowchart displaying the main decision made during the classification is given (Fig. 3). While our classification method still contains a subjective factor, our opinion is that it presents an improvement over previous methods (e.g. Mäkelä *et al*. 2000b, Kulmala *et al*. 2001b). In these papers, the classification was based on the strength and visual distinction of the new particle mode. The main improvement in our method is the clear distinction between days with no particle formation and days containing a particle formation burst. The most problematic days, for example days with small particles appearing sporadically or days with a new mode starting to

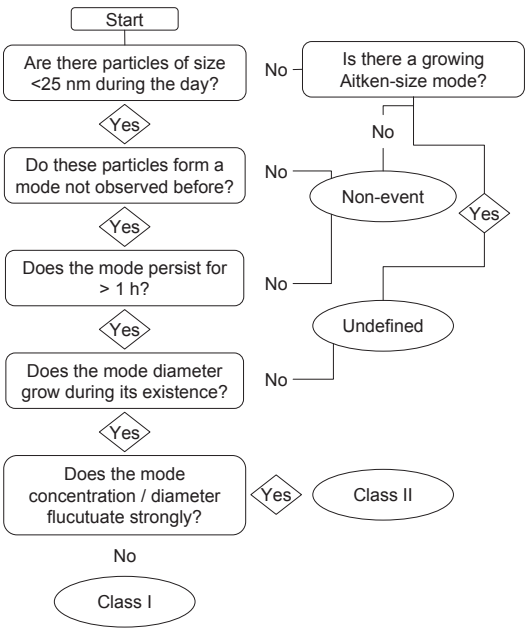

Fig. 3. A flowchart of the decision path during the classification of the daily size distributions.

grow in the Aitken size range, are classified as undefined and thus withdrawn from the analysis comparing event and non-event days. In short: while we were not able to define a definitive set of criteria for a NPF event, our methods improve on the previous ones by reducing the chance of misclassification.

Log-normal fitting

As we previously stated, the size distributions measured at the SMEAR II station exhibit several log-normally distributed modes. It is often convenient and mathematically straightforward to use a modal representation of the size distribution, where the distribution is described as the sum of i modes with parameters D_{pg} (geometric mean diameter), σ_i (geometric standard deviation) and N_i (number concentration). To find these parameters for the experimentally measured size distributions we used an automated fitting method that has recently been developed at the University of Helsinki (Hussein *et al*. 2005). The fitting program analyzes the measured size distribution to decide the number of modes to fit, makes a starting guess of the modal parameters, and then uses a least-square minimization method to fit 2–3 modes to the measured size distribution. It then returns parameters of the log-normal modes found. The analysis method takes into account the modal structure before the measurement time, which emphasizes a continuous modal structure. In Fig. 1, we display the lognormal modes obtained with the automated fitting method along with the measured size distribution data.

Growth rate and nucleation rate derivation

A critical part of the NPF event is the condensational growth of new particles to larger sizes, due to several factors:

i. the growth process increases the size of the new particles so that they are less prone to removal by inter- and intramodal coagulation,
ii. the growth of these new particles might eventually progress to Aitken- and even accumulation mode sizes, where they are likely to participate in cloud formation processes,
iii. the condensation growth removes condensable vapors from the atmosphere, which may be a control mechanism suppressing further particle formation.

Our aim was to derive the rate at which the newly formed aerosol population grows, $dD_{p,nuc}/dt$. In the literature several detailed ways of deriving the growth and formation rates can be found (e.g. Weber *et al*. 1995). For the SMEAR II data we needed a robust method, which copes well with fluctuating data and is straightforward to use. Previous studies of the SMEAR data used the maximum size that the nucleation mode particles reached by the end of the event as the basis of the growth rate determination (Mäkelä *et al*. 2000a). Another method involved visual determination of the mode size change (Kulmala *et al*. 2001a). Both methods relied strongly on user input, and gave results with a large error range.

A straightforward way to determine the growth rate would be to follow the temporal change of the mean diameter or the geometric mean diameter. However, this presented us with the problem of defining the limits over which to average. If the averaging is performed over a range containing large particles (> 20 nm), the result is influenced by pre-existing particles. On the other hand, if the range is limited only to small particles and the growth rate is large, it may happen that the particles grow quickly out of the averaging range and our parameter does not represent the new population in its entirety.

The modal geometric mean D_{pg}, which we obtained as a result of the fitting procedure, is, however, a good choice for growth rate analysis. In a log-normally distributed population D_{pg} is also the median diameter (Seinfeld and Pandis 1998), meaning that the majority of the particles are of a size close to D_{pg}.

To obtain the growth rate, we fitted a first-order polynomial to the geometric mean diameters of the nucleation mode during the formation burst (Fig. 4, upper panel). If the new particle mode was not well-behaved over the whole time period that it was visible, we chose a time period where

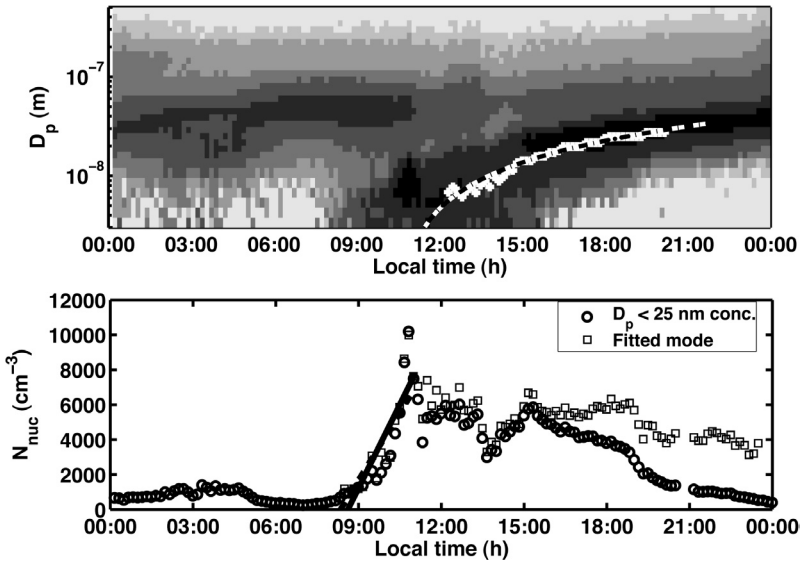

Fig. 4. Example of the event analysis and its results. In the upper panel, we present a surface plot of a new particle formation burst. White dots mark the geometric mean diameter of the nucleation mode (obtained by the fitting procedure), and the gray line represents the first-order polynomial fit result, from which we get the particle growth rate. The lower panel contains the nucleation mode particle concentration as a function of time, taken from the log-normal fitting procedure as well as the number of < 25 nm particle concentration. The solid lines show the first-order polynomial fit result, which was used to obtain dN_{nuc}/dt.

the growth was close to constant, preferring to use a time period close to the beginning of the burst.

We additionally tried a method described by Lehtinen and Kulmala (2003), where the evolution of the new mode is determined by following the concentration of each "channel" (mobility size range) of the DMPS. In this method, we identify the peak in each channel caused by the mode passing its size range; we used a normal distribution fit to identify the peak. By recording the instants in time when each peak is recorded, we can then derive the growth rate. This method, while being efficient for sub-10-nm particles (e.g. Hirsikko *et al*. 2005), proved ill suited for our analysis. The logarithmically spaced channels caused a broadening of the peaks, making it difficult to identify the exact time of peak passage at larger particle sizes. Additionally, the method is sensitive to fluctuations in the mode concentration, which is usual in our data, requiring careful user input to select the correct peak.

The formation rate of new particles is more difficult to derive because the DMPS system cannot measure particles smaller than 3 nm in size. Therefore, we focused on the flux of particles into the observable size range. Because no information is available of the temporal behavior of the real formation rate, we assume a constant particle source that is active during a time period $[t_{1,start},t_{1,end}]$. The produced particles then appear in the observable size range between the times $t_{2,start}$ and $t_{2,end}$, where the time difference $t_{2,start} - t_{1,start}$ depends on the growth rate of the freshly formed particles. During this time, a fraction of the particles are lost due to coagulation processes. The flux of particles into the observable size range, J_{nuc}, can be calculated from the following equation (*see* for example Kulmala *et al*. 2004 and references therein):

$$J_{nuc} = dN_{nuc}/dt + F_{coag} + F_{growth} \quad (1)$$

where N_{nuc} is the nucleated particle concentration, F_{coag} is the loss of particles due to coagulation and F_{growth} is the flux of particles out of the size range. We chose the size range for the nucleated particles (N_{nuc}) to be from 3 nm up to 25 nm, allowing us to neglect the growth term in Eq. 1, as particles rarely grew over this size before formation ended. Smaller ranges could be used

to gain insight into the time dependence of the formation rate; however, our aim was to obtain a more general average formation rate, so a more stable size range was used.

In some cases the particles grew out of the 3–25 nm range; to analyze these cases we also calculated N_{nuc} from the fitted modal concentration of the nucleation mode. The concentration was generally equal to the concentration in the 3–25 nm size range. However, when the formed particles grew fast, F_{growth} could no longer be neglected due to growth out of the range and the fitted mode contained more particles than the 3–25 nm range. The formation rate was calculated using both methods (integration over 3–25 nm and fitted concentration) for determining N_{nuc}. The results presented in this paper are calculated with the integration method; in cases where they contained a large error due to the mode growing quickly out of the 3–25 nm size range, the modal rate was used. If both methods failed, for example due to bad fitting results at lower mode sizes, the day was classified as class II.

To calculate dN/dt, we determined $t_{2,start}$ and $t_{2,end}$ by choosing the period when the particle number showed a linear increase (Fig. 4, lower panel). We then fitted a first-order polynomial to the values of N_{nuc}. F_{coag} was calculated from

$$F_{coag} = \mathrm{CoagS}_{nuc} N_{nuc} \quad (2)$$

where CoagS_{nuc} is the coagulation sink of particles in the nucleation mode. The reference size for CoagS_{nuc} was taken to be the GMD of the fitted nucleation mode. A mean value of F_{coag} over the observed formation period was taken. The magnitude of F_{coag} is usually of the same order than the observed dN/dt.

Condensation and coagulation sink

To quantify condensation and coagulation processes during new particle formation, it is of use to calculate the condensation sink and the coagulation sinks (*see* for example Kulmala *et al.* 2001a). The condensation sink is defined as

$$\begin{aligned} \mathrm{CS} &= 2\pi D \int D_p \beta_m(D_p) n(D_p) dD_p \\ &= 2\pi D \sum \beta_m(D_{p,i}) D_{p,i} N_i \end{aligned} \quad (3)$$

where $D_{p,i}$ is the diameter of a particle in size class i and N_i is the particle concentration in the respective size class. D is the diffusion coefficient of the condensing vapor. We used the transition regime correction factor β_m from Fuchs and Sutugin (1970). CS describes the ability of the size distribution to remove condensable vapors from the atmosphere. In practice, the vapor was assumed to have a very low vapor pressure at the surface of the particle, and molecular properties similar to sulfuric acid. The coagulation sink for a particle of size i is defined as

$$\mathrm{CoagS}(D_p) = \int K(D_p', D_p) n(D_p') dD_p' \quad (4)$$

where K is the coagulation coefficient (kernel) of particles with sizes D_p and D_p', calculated by using the formula of Fuchs (1964) (*see* e.g. Seinfeld and Pandis 1998). Both these parameters are strongly dependent of the number size distribution. Because the DMPS system at the SMEAR II station measures the size distribution of dried particles, the measurement does not represent ambient conditions. The sink values are proportional to D_p^{μ}, where μ ranges from 1 to 2, making the sinks sensitive to particle diameter changes. The measured size distributions were corrected for hygroscopic growth according to (Laakso *et al.* 2004):

$$\mathrm{GF}(D_p, \mathrm{RH}) = (1 - \mathrm{RH}/100)^{\gamma}. \quad (5)$$

Here GF is the growth factor of a particle of size D_p in a relative humidity RH. γ is a parameter derived by a least-square fit to hygroscopicity data measured during the BIOFOR campaign in Hyytiälä (Hämeri *et al.* 2001), given by $\gamma = -3.1116 \times 10^5 \times D_p - 0.0847$. The GF was restricted so that it could not exceed the GF of ammonium sulphate.

Using this parameterization increased the CS value usually by a factor between 1.1 and 2.0, with a mean and median of 1.62 and 1.48, respectively.

From the growth rate and the condensation sink it is possible to derive estimates for the condensing vapor concentration C_v and its source rate Q following the analysis by Kulmala *et al.* (2001a) and Dal Maso *et al.* (2002), which is summarized in the following. Assuming that the particle growth is caused by condensation of a

low vapor pressure vapor to the particle surface we can integrate the mass flux equation to derive C_v according to (Kulmala 1988). In the nucleation size range this leads to a simple approximate relation between the growth rate and the vapor concentration:

$$C_v = A \times dD_p/dt. \quad (6)$$

Here A is a constant, which has the value 1.37×10^7 h cm^{-3} nm^{-1} for a vapor with molecular properties of sulfuric acid. Thus, a growth rate of 1 nm h^{-1} corresponds to a vapor concentration of 1.37×10^7 cm^{-3}.

Assuming no other sink terms for the condensing vapor, the time dependence of the condensing vapor follows the differential equation

$$dC_v/dt = Q - \mathrm{CS} \times C_v. \quad (7)$$

If the changes in the source rate are slow as compared with the value of CS^{-1} (the characteristic lifetime of the vapor), we can assume a steady-state situation and set the left side of (Eq. 7) to zero. This leads to the equation

$$Q = \mathrm{CS} \times C_v = \mathrm{CS} \times A \times dD_p/dt. \quad (8)$$

Results

Event statistics

Our dataset comprised 2892 days. A total of 699 events were found during the eight-year time period (Table 1), meaning that on average every fourth day (24.2%) contained an event. Non-events amounted to 29.3% of the days, and the rest of the days (46.5%) were either classified as undefined or contained bad or missing data. If we consider only the days when either an event or non-event was recorded as classified days, the event fraction rises to 45.2% of the data.

Event occurrence had a clear annual variation pattern (Fig. 5). The number of events was highest in the spring months (March–May), with 344 (49%) of the events occurring during this period. During this time we observed particle formation on 48% of all days. In autumn we found a maximum of event frequency around September. During the winter months (November–February) only 8% of the days were particle formation days.

The non-event yearly distribution exhibits inverse behavior as compared with that of the the events, with maxima in winter and summer months. Undefined days are fewer during March–June and September (ca. 30% of all days), while during the rest of the year their percentage varies between 40% and 50%.

The number of events per year was also studied to find whether particle formation exhibited long-term variability (Fig. 6). The number of events decreased from 1996–1998, but since then increased from 64 yearly event days in 1998 to 121 in 2003. The year 2002 is the first year when the number of events is greater than the non-event number. The yearly amount of undefined days stays fairly constant, varying between 35% and 45% of all days with data. Of the 699 event days, 334 (47%) contained data that was fit for analysis of the burst characteristics. In the following section we present these characteristics.

Event characteristics

The mean growth rate of the nucleation mode particles in our data was 3.0 nm h^{-1} and the median was 2.5 nm h^{-1}. The annual variation (Fig. 7, upper panel) showed an increase of nucleation mode growth rate towards summer, when the growth rates were generally clearly

Table 1. Event statistics.

	Days	Percentage of all days	Percentage of classified days*
Class I	334	11.5	21.5
Class Ia	79	2.7	5.1
Class II	365	12.6	23.6
Total events	699	24.2	45.2
Non-events	848	29.3	54.8
Undefined	1078	37.3	
Not classifiable	267	9.2	
Total days	2892		
Of which classified*	1547		

*Classified days include days classified either as event days or non-event days.

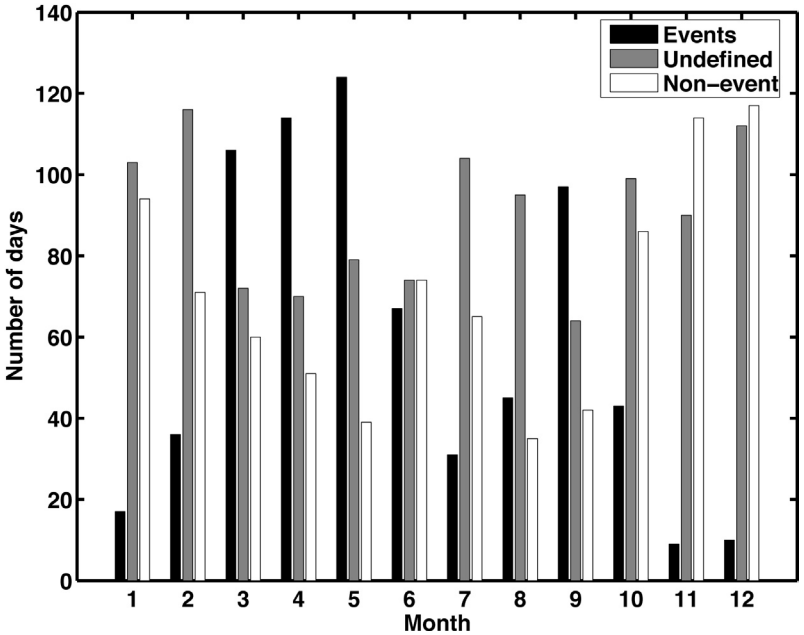

Fig. 5. The total number of event days, non-event days and undefined days during each month of the year at the SMEAR II station, Hyytiälä, Finland during 1996–2003.

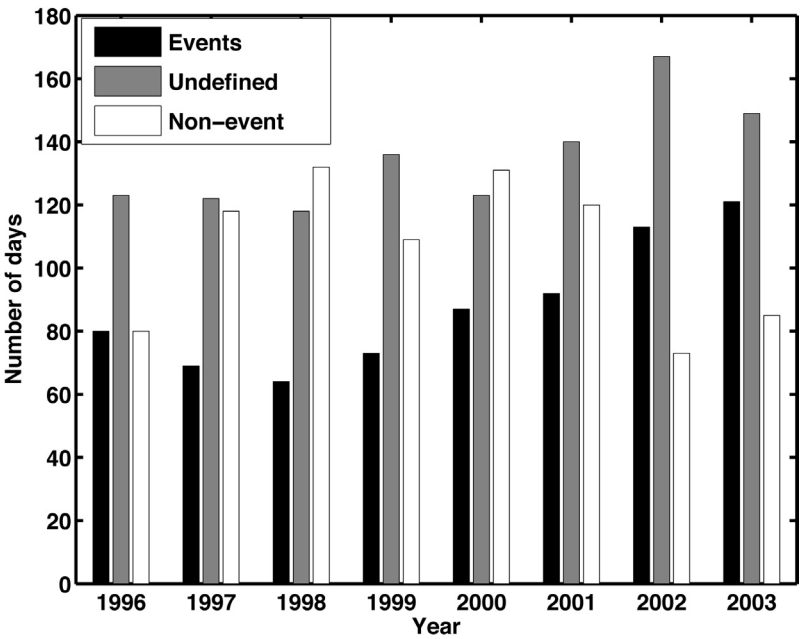

Fig. 6. The total number of event days, non-event days and undefined days during each year at the SMEAR II station, Hyytiälä, Finland during 1996–2003.

over the mean. Spring and autumn events had growth rates around the average value, while winter events exhibited low growth rates.

The mean appearance rate of larger than 3 nm particles, J_{nuc}, was 0.8 cm^{-3} s^{-1}, varying from 0.06 to 5 cm^{-3} s^{-1}. The annual variation (Fig. 7, lower panel) shows a similar pattern to the event occurrence: formation rates are high during spring, lower during summer and a smaller maximum can be seen around September. In spring, very high formation rates could be observed. The contribution of the coagulation loss flux F_{coag} was on average between 20% and 40% of the total appearance rate, meaning that the directly observable formation rate was only ca. 70% of the real appearance rate.

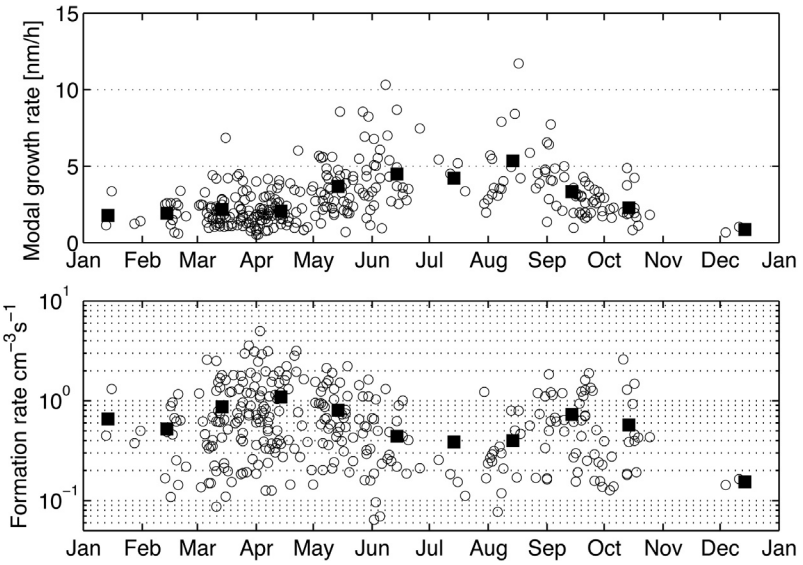

Fig. 7. Upper panel: The new particle diameter growth rates as a function of the day of year in Hyytiälä, 1996–2003. Lower panel: Formation rate (J_{nuc}) as a function of the day of year. The black squares represent the monthly mean values. The values have been calculated for class I event days.

The average condensation sink during the growth period was 2.4×10^{-3} s^{-1}, corresponding to a characteristic vapor lifetime of about 7 minutes (Fig. 8, upper panel). For comparison, we calculated the average condensation sink during non-event days, which was 7.0×10^{-3} s^{-1}. The annual variation of the condensation sink during events is small except for wintertime, when the few events that were observed had very low condensation sinks.

The vapor source rate (Fig. 8, lower panel) varied between 10^4 and 10^6 cm^{-3}. The annual variation is similar to the growth rate, with a maximum during the summer months. Events occurring during winter had the lowest source rates of all the events.

In Table 2, we present a summary of the monthly means of the event characteristics and the mean condensation sink during non-event days.

Discussion

Based on our data, it is clear that new particle formation bursts are a frequent phenomenon in the boreal forest boundary layer. The minimum fraction of days that are events was 24.2%. How-

Table 2. Monthly means of event characteristics. GR is the growth rate, J_{nuc} is the appearance rate of particles, CS(events) is the condensation sink during the events, CS(non-events) is the condensation sink for non-events and Q is the vapor source rate.

Month	GR (nm h^{-1})	J_{nuc} (cm^{-3} s^{-1})	CS(events) (10^{-3} s^{-1})	CS(non-events) (10^{-3} s^{-1})	Q (10^3 cm^{-3} s^{-1})
Jan	1.8	0.7	0.9	5.3	25.2
Feb	1.9	0.5	2.4	6.9	66.5
Mar	2.2	0.9	2.3	8.5	62.7
Apr	2.1	1.1	2.5	10.2	71.7
May	3.7	0.8	3.5	8.2	127.5
Jun	4.5	0.4	2.5	7.4	207.5
Jul	4.2	0.4	2.5	8.1	154.1
Aug	5.3	0.4	2.2	5.9	180.4
Sep	3.3	0.7	1.9	9.5	90.7
Oct	2.3	0.6	1.7	6.2	53.2
Nov	N/A	N/A	N/A	5.6	N/A
Dec	0.9	0.2	0.5	5.8	6.0

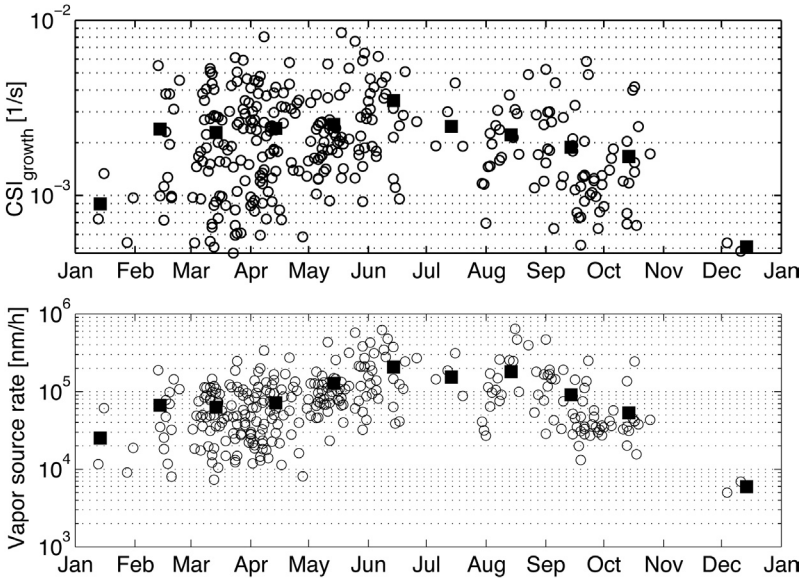

Fig. 8. Upper panel: The average condensation sink value during the growth periods of class I event days as a function of the day of year in Hyytiälä, Finland 1996–2003. Lower panel: The calculated vapor source rate of class I events. Black squares represent monthly mean values.

ever, considering the number of undefined days it is likely that the real fraction was greater. If, for example, we make a conservative guess and assume that 20% of the undefined days are in reality event days, the event fraction would rise to 32%, almost a third of all days.

The annual variation of the event frequency has been reported earlier for the boreal forest (Mäkelä *et al*. 2000b, Vehkamäki *et al*. 2004). The low number of events in winter suggests that solar irradiation and temperature play a role in the particle formation process, with biogenic precursor vapors also having an influence. The event minimum in summer, however, points to additional factors, possibly air mass origin (*see* Sogacheva *et al*. (2005) for a detailed study) or biogenic VOC emissions by trees (Hakola *et al*. 2003). The increase in the number of events during the recent years is a new result, and further study is needed to shed light on the reasons for this increase.

The annual patterns of the formation and growth rates are similar to ones reported by Mäkelä *et al*. (2000b), but the formation rates are higher. This is partly due to the coagulation loss correction made, and partly because a different methodology used to derive the formation rate. The growth rate maximum in summer together with the vapor source rate variation suggests that the condensable species is much more readily available during warm periods of the year (Hirsikko *et al*. 2005). The difference in the annual pattern of the formation and growth rates suggests that the process acting as a particle source is different from the one growing the new aerosol.

Based on our event classification and calculation of event characteristics, we can roughly divide the year into periods according to the type of events found in these periods:

- Winter (Nov–Feb): Events occur very rarely. When observed, they display low growth and formation rates, as well as low condensation sink values during the growth period. The vapor source rate is very small.
- Spring (March–May): Events occur often. They have a high formation rate and a moderate growth rate, but the condensation sink during events is around the event mean value. The vapor source rate is of moderate strength.
- Summer (June–mid-August): Events are not frequently observed. The new particles grow fast, but the observed formation rate is low. The condensation sink during the events is slightly higher than usual, as well as the source rate.
- Autumn (mid-August–October): Frequency and formation rates are generally less high.

Conclusions

We have used a simple classification scheme to find new particle formation events in the exceptionally long eight-year time series of atmospheric aerosols number size distributions measured at the SMEAR II station in Hyytiälä, Finland. The event classification method was chosen so that the misclassification of days was minimized, and only clear instances of particle formation were included. Our analysis revealed that events are almost as frequent as clear non-events in the boreal forest environment. Event frequency is highest in spring, with minima during winter and summer, which is in concordance with previous studies.

We also classified the event days when it is possible to quantify the rate of particle formation and growth. These parameters, in addition to the condensation sink and vapor source rate, were derived for a statistically significant number (334) of days in our dataset using methodology that is more reliable than the methods used in our earlier studies (*see* for example Mäkelä *et al*. 2000b). Our method for calculating the burst characteristics is simple and physically well justified, leading to reproducible data for comparison with modeling efforts or measurements from other measurement sites.

Growth rates observed in our dataset are of the same order as reported in the literature at other sites, with similar annual variation (Kulmala *et al*. 2004). Appearance rates of new particles were also of the order of 1.0 cm^{-3} s^{-1}, which is a rate often observed in atmospheric conditions and also previous studies of the SMEAR II data.

The database of event and non-event days and the event characteristics forms the basis of future studies into the causes and effects of atmospheric particle formation in the boreal forest. The database enables detailed air mass origin analysis, as well as statistical analysis of aerosol data and other physical, chemical and biological data measured at the SMEAR II site. Using the guidelines for event classification described here for other sites with long-term aerosol size distribution measurements will help in studying the climatic relevance and magnitude of atmospheric new particle formation.

Acknowledgements: M. Dal Maso wishes to thank the Maj and Tor Nessling foundation for financial support of this study.

References

Aalto P., Hämeri K., Becker E., Weber R., Salm J., Mäkelä J.M., Hoell C., O'Dowd C.D., Karlsson H., Hansson H.-C., Väkevä M., Koponen I.K., Buzorius G. & Kulmala M. 2001. Physical characterization of aerosol particles during nucleation events. *Tellus* 53B: 344–358.

Birmili W. & Wiedensohler A. 2000. New particle formation in the continental boundary layer: Meteorological and gas phase parameter influence. *Geophys. Res. Lett.* 27: 3325–3328.

Boy M. & Kulmala M. 2002. Nucleation events in the continental boundary layer: Influence of physical and meteorological parameters. *Atmos. Chem. Phys.* 2: 1–16.

Dal Maso M., Kulmala M., Lehtinen K.E.J., Mäkelä J.M., Aalto P. & O'Dowd C.D. 2002. Condensation and coagulation sinks and formation of nucleation mode particles in coastal and boreal forest boundary layers. *J. Geophys. Res.* 107(D19), doi:10.1029/2001JD001053.

Fuchs N.A. 1964. *The mechanics of aerosols*. Pergamon, New York.

Fuchs N.A. & Sutugin A.G. 1970. *Highly dispersed aerosols*. Ann Arbour Science Publishers, Ann Arbour, London.

Hakola H., Tarvainen V., Laurila T., Hiltunen V., Hellen H. & Keronen P. 2003. Seasonal variation of VOC concentrations above a boreal coniferous forest. *Atmos. Environ.* 37: 1623–1634.

Hämeri K., Väkevä M., Aalto P.P., Kulmala M., Swietlicki E., Zhou J., Seidl W., Becker E. & O'Dowd C.D. 2001. Hygroscopic and CCN properties of aerosol particles in boreal forests. *Tellus* 53B: 359–379.

Hari P. & Kulmala M. 2005. Station for Measuring Ecosystem–Atmosphere Relations (SMEAR II). *Boreal Env. Res.* 10: 315–322.

Hirsikko A., Laakso L, Hõrrak U., Aalto P.P., Kerminen V.-M. & Kulmala M. 2005. Annual and size dependent variation of growth rates and ion concentrations in boreal forest. *Boreal Env. Res.* 10: 357–369.

Hussein T., Dal Maso M., Petäjä T., Koponen I.K., Paatero P., Aalto P.P., Hämeri K. & Kulmala M. 2005. Evaluation of an automatic algorithm for fitting the particle number size distributions. *Boreal Env. Res.* 10: 337–355.

Jokinen V. & Mäkelä J.M. 1997. Closed loop arrangement with critical orifices for DMA sheath/excess flow system. *J. Aerosol Sci.* 28: 643–648.

Koponen I., Virkkula A. Hillamo R., Kerminen V.-M. & Kulmala M. 2003. Number size distributions and concentrations of the continental summer aerosols in Queen Maud Land, Antarctica. *J. Geophys. Res.* 108(D18), doi:10.1029/2002JD002939.

Kulmala M. 1988. *Nucleation as an aerosol physical problem*. Ph.D. thesis, University of Helsinki.

Kulmala M., Toivonen A., Mäkelä J.M. & Laaksonen A. 1998. Analysis of the growth of nucleation mode particles in boreal forest. *Tellus* 50B: 449–462.

Kulmala M., Vehkamäki H., Petäjä T., Dal Maso M., Lauri A., Kerminen V.-M., Birmili W. & McMurry P. 2004. Formation and growth rates of ultrafine atmospheric particles: a review of observations. *J. Aerosol Sci.* 35: 143–176.

Kulmala M., Dal Maso M., Mäkelä J.M., Pirjola L., Väkevä M., Aalto P., Miikkulainen P., Hämeri K. & O'Dowd C.D. 2001a. On the formation, growth and composition of nucleation mode particles. *Tellus* 53B: 479–490.

Kulmala M., Hämeri K., Aalto P.P., Mäkelä J.M., Pirjola L., Nilsson E.D., Buzorius G., Rannik Ü., Dal Maso M., Seidl W., Hoffmann T., Janson R., Hansson H.-C., Viisanen Y., Laaksonen A. & O'Dowd C.D. 2001b. Overview of the international project on biogenic aerosol formation in the boreal forest (BIOFOR). *Tellus* 53B: 324–343.

Laakso L., Petäjä T., Lehtinen K., Kulmala M., Paatero J., Hõrrak U., Tammet H. & Joutsensaari J. 2004. Ion production rate in a boreal forest based on ion, particle and radiation measurements. *Atmos. Chem. Phys.* 4: 1933–1943.

Lehtinen K. & Kulmala M. 2003. A model for particle formation and growth in the atmosphere with molecular resolution in size. *Atmos. Chem. Phys.* 3: 251–258.

Mäkelä J.M., Koponen I.K., Aalto P. & Kulmala M. 2000a. One year data of submicron size modes of tropospheric background aerosols in southern Finland. *J. Aerosol Sci.* 31: 596–611.

Mäkelä J.M., Dal Maso M., Pirjola L., Keronen P., Laakso L., Kulmala M. & Laaksonen A. 2000b. Characteristics of the atmospheric particle formation events observed at a boreal forest site in southern Finland. *Boreal Env. Res.* 5: 299–313.

Mäkelä J.M., Aalto P., Jokinen V., Pohja T., Nissinen A., Palmroth S., Markkanen T., Seitsonen K., Lihavainen H. & Kulmala M. 1997. Observations of ultrafine aerosol particle formation and growth in boreal forest. *Geophys. Res. Lett.* 24: 1219–1222.

Mönkkönen P., Koponen I., Lehtinen K., Hämeri K., Uma R. & Kulmala M. 2005. Measurements in a highly polluted Asian mega city: Observations of aerosol number size distributions, modal parameters and nucleation events. *Atmos. Chem. Phys.* 5: 57–66.

O'Dowd C.D., Hämeri K., Mäkelä J.M., Pirjola L., Kulmala M., Jennings S.G., Berresheim H., Hansson H.-C., de Leeuw G., Kunz G.J., Allen A.G., Hewitt C.N., Jackson A., Viisanen Y. & Hoffmann T. 2002. A dedicated study of New Particle Formation and Fate in the Coastal Environment (PARFORCE): Overview of objectives and achievements. *J. Geophys. Res.* 107(D19), 8108, doi:10.1029/2001JD000555.

Seinfeld J.H. & Pandis S.N. 1998. *Atmospheric chemistry and physics: from air pollution to climate change*, John Wiley and Sons, New York.

Sogacheva L., Dal Maso M., Kerminen V.-M. & Kulmala M. 2005. Probability of nucleation events and aerosol particle concentration in different air mass types arriving at Hyytiälä, Southern Finland, based on back trajectories analysis. *Boreal Env. Res.* 10. [In press].

Vehkamäki H., Dal Maso M., Hussein T., Flanagan R., Hyvärinen A., Lauros J., Merikanto J., Mönkkönen P., Pihlatie M., Salminen K., Sogacheva L., Thum T., Ruuskanen T., Keronen P., Aalto P., Hari P., Lehtinen K. & Kulmala M. 2004. Atmospheric particle formation events at Värriö measurement station in Finnish Lapland 1998–2002. *Atmos. Chem. Phys.* 4: 2015–2023.

Vesala T., Haataja J., Aalto P., Altimir N., Buzorius G., Garam E., Hämeri K., Ilvesniemi H., Jokinen V., Keronen P., Lahti T., Markkanen T., Mäkelä J.M., Nikinmaa E., Palmroth S., Palva L., Pohja T., Pumpanen J., Rannik Ü., Siivola E., Ylitalo H., Hari P. & Kulmala M. 1998. Long-term field measurements of atmosphere–surface interactions in boreal forest ecology, micrometeorology, aerosol physics and atmospheric chemistry. *Trends in Heat, Mass and Momentum Transfer* 4: 17–35.

Weber R.J., McMurry P.H., Eisele F.L. & Tanner D.J. 1995. Measurements of expected nucleation precursor species and 3–500-nm diameter particles at Mauna Loa observatory, Hawaii. *J. Atmos. Sci.* 52: 2242–2257.

Received 13 April 2005, accepted 1 July 2005